Thermal and mechanical properties of PLA/ENR thermoplastic vulcanizates compatibilized with tetrafunctional double-decker silsesquioxanes

Sandra Paszkiewicz[1), *)] (ORCID ID: 0000-0001-7487-9220), **Grzegorz Kramek**[1)] (0000-0002-8671-8739), **Konrad Walkowiak**[1)] (0000-0001-8629-7367), **Izabela Irska**[1)] (0000-0002-5521-1847), **Elżbieta Piesowicz**[1)] (0000-0003-4371-5236), **Monika Rzonsowska**[2)] (0000-0002-4739-070X), **Beata Dudziec**[2)] (0000-0001-6344-0298), **Mateusz Barczewski**[3)] (0000-0003-1451-6430)

DOI: https://doi.org/10.14314/polimery.2023.11.3

Abstract: The influence of the addition of tetrafunctional double-decker silsesquioxanes (DDSQ-ether-4OH) on the compatibility, thermal and mechanical properties of polylactide and epoxidized natural rubber (PLA/ENR) vulcanizates was investigated. The apparent cross-linking density and thermal stability of PLA/ENR vulcanizates were also determined. The FTIR analysis confirmed the compatibilizing effect of DDSQ-ether-4OH and the formation of the PLA-g-ENR copolymer. A strong effect of ENR content and DDSQ-ether-4OH addition on the thermal and mechanical properties of the obtained vulcanizates was demonstrated.

Keywords: polylactic acid, epoxidized natural rubber, dynamic vulcanization.

Właściwości termiczne i mechaniczne termoplastycznych wulkanizatów PLA/ENR kompatybilizowanych czterofunkcyjnym silseskwiokanem typu double-decker

Streszczenie: Zbadano wpływ dodatku czterofunkcyjnego silseskwioksanu typu *double-decker* (DDSQ-eter-4OH) na kompatybilność oraz właściwości termiczne i mechaniczne wulkanizatów polilaktydu i epoksydowanego kauczuku naturalnego (PLA/ENR). Oznaczono również pozorną gęstość usieciowania i stabilność termiczną wulkanizatów PLA/ENR. Metodą FTIR potwierdzono kompatybilizujące działanie DDSQ-eter-4OH i utworzenie kopolimeru PLA-g-ENR. Wykazano silny wpływ zawartości ENR i dodatku DDSQ-eter-4OH na właściwości termiczne i mechaniczne otrzymanych wulkanizatów.

Słowa kluczowe: polilaktyd, epoksydowany kauczuk naturalny, dynamiczna wulkanizacja.

The growing focus on utilizing polymeric materials sourced from renewable resources is driven by the increasing environmental consciousness of society and worries about the depletion of petrochemical-based material [1]. Polylactide (PLA) has gained popularity as a sustainable material for bio-based products because it originates from aliphatic polyester, which offers excellent biodegradability and biocompatibility. Furthermore, PLA exhibits high strength and stiffness, making it a promising substitute for petroleum-based materials [2]. Regrettably, the natural brittleness of PLA has been a significant limitation in its potential applications. Consequently, various efforts have been undertaken to enhance PLA's toughness, including copolymerization [3–5], plasticization [6, 7], blending [5, 8, 9], and the development of filled composites [10–14].

The most practical and cost-effective approach to enhancing the toughness of PLA is achieved by blending it with other polymers. Elastomers' addition and blending are often regarded as an effective method for improving amorphous thermoplastics' ductility and impact strength. Elastomeric particles function as stress concentrators, increasing the ability of brittle polymers by absorbing fracture energy and resulting in a more durable material. PLA has been blended with various elastomers, including thermoplastic polyurethane (TPU)

[1)] West Pomeranian University of Technology, Faculty of Mechanical Engineering and Mechatronics, Department of Materials Technologies, Piastow Av. 19, 70-310 Szczecin, Poland.

[2)] Adam Mickiewicz University in Poznan, Faculty of Chemistry and Centre for Advanced Technologies, Uniwersytetu Poznanskiego 8–10, 61-614 Poznan, Poland.

[3)] Poznan University of Technology, Faculty of Mechanical Engineering and Management, Institute of Materials Technology, Polymer Processing Division, Piotrowo 3, 61-138 Poznan, Poland.

[*)] Author for correspondence: spaszkiewicz@zut.edu.pl

[15], polyurethane [16], poly(ethylene-glycidyl methacrylate) (EGMA) [11], polyamide elastomer (PAE) [17], poly(ether-*b*-amide) copolymer (PEBA) [18], ethylene-propylene-diene-rubber (EPDM) [19] etc. Although these elastomers have indeed increased the toughness of PLA, most of them are synthetic materials derived from petroleum-based sources.

Natural rubber (NR) is an environmentally sustainable resource obtained from the latex of rubber trees. Its unique combination of toughness, biocompatibility, and biodegradability, coupled with its bio-based origins, renders it a perfect choice for addressing the brittleness of PLA [20]. Several studies report about NR toughing PLA [20–23]. Bitinis *et al*. [20–22] analyzed in detail PLA/NR blends. Their research revealed that 10 wt% is the ideal concentration of NR for significantly enhancing the toughness of PLA. In the blends, a phase-separated structure was observed, with NR forming small droplets dispersed within the continuous PLA phase. Juntuek [23] similarly discovered that the blend of PLA/NR achieved its maximum impact strength when using a 90/10 (PLA/NR) wt. ratio. To enhance compatibility in the PLA/NR blend, they incorporated glycidyl methacrylate-grafted natural rubber (NR-*g*-GMA), resulting in the dispersion of NR domains within the PLA matrix. In addition, Xu *et al*. [24] reported a super toughened dynamically vulcanized PLA/NR blend in which the cross-linked NR had a continuous phase and excellent interfacial compatibility with PLA.

It is widely recognized that elastomers should be evenly dispersed as small domains within the polymer matrix to enhance the toughness of polymers. Furthermore, numerous investigations of PLA/NR blends have highlighted the issue of inadequate compatibility between these polymers. One approach to address this issue involves incorporating epoxidized natural rubber [25–27] and its derivatives [28–30], employing functional modifiers during the reaction mixing [31, 32], and pretreating NR to enhance the presence of oxygen-containing groups [31, 33]. However, it is important to note that these techniques necessitate using costly materials. Commercial PLA and its blends have been modified by the wide spectrum of plasticizers and compatibilizers.

Recent research has extensively employed polyhedral oligomeric silsesquioxanes (POSS) to prepare polymer nanocomposites [34, 35]. Among all nanofillers, POSS is characterized as zero-dimensional. Typically, POSS particles measure between 0.6 and 1.2 nanometers in diameter and may contain certain functional groups [36]. There are considerable reports on the use of POSS molecules to function as a coagent [36] or compatibilizer [37–42] and improve thermal resistance [43, 44] mechanical properties [45] and flame retardancy [46, 47] of resulting hybrid materials. However, the usage of POSS as a compatibilizer is particularly interesting. For instance, Zhao *et al*. [40] investigated the thermal and mechanical properties of octavinyl-polyhedral oligomeric silsesquioxanes (OV-POSS)/NR blends. The authors prepared five different blends with a content of 5, 10, 15, and 20 phr OV-POSS. They revealed vinyl groups of OV-POSS partially acted as vulcanizing agents, and the addition of POSS led to an improvement in thermal stability. The research also examined the transport properties of POSS/NR composites using different forms of POSS, and it was determined that the inclusion of POSS enhanced the resistance of the NR matrix to solvents [48]. Kalkan *et al*. [41] investigated octavinyl silsesquioxanes (OV-POSS) incorporation into natural rubber (NR)/butadiene rubber (BR) elastomer blends as a potential compatibilizer. Additionally, Kilic *et al*. [42] used epoxidized polyhedral oligomeric silsesquioxanes (epoxy-POSS) as a successful compatibilizer in poly(lactic acid) (PLA)/poly(butylene adipate-*co*-terephthalate) (PBAT) blends. Three different epoxy-POSS types were utilized, having one-, tri-, and multi-epoxides per POSS cage. The compatibilization of PLA and PBAT was shown through the decrease in the size of dispersed particles and the shifts in the glass transition temperatures of phases. Mechanical properties of PLA/PBAT improved in the presence of epoxy-POSS systems. This research group [38] has also checked the effect of molecular weight of poly(butylene adipate-co-terephthalate) (PBAT) on the immiscible poly(lactic acid) (PLA)/PBAT blends compatibilized with epoxidized silsesquioxanes having different numbers of epoxy groups per molecule (epoxy-POSSs). Mechanical tests revealed all epoxy-POSS types significantly improved the performance of the blends containing low-molecular-weight PBAT. In other immiscible systems, polyhedral oligomeric silsesquioxanes (POSS) copolymer was used as a compatibilizer between poly(methyl methacrylate) (PMMA) and polystyrene (PS) [39]. It was found that the presence of isobutyl units on the corners of POSS cage is clearly sufficient to encourage miscibility with PMMA. Within the family of polyhedral oligomeric silsesquioxanes, a new class of the so-called double-decker (DDSQ) type of silsesquioxanes has attracted attention. Studies on the synthesis and use of this DDSQ system involve the utility of the "closed" and "open" core derivatives, and refer to di- and tetrafunctionalized DDSQ compounds, respectively. This in turn affects the application of these systems in the formation of macromolecular DDSQ-based hybrid materials [49, 50].

In the present study, double-decker silsesquioxanes (DDSQ-eter-4OH) with dedicated functional hydroxyl groups as a compatibilizer in the eco-friendly PLA/epoxidized NR (ENR) system was used. This work aimed to investigate two key factors: the influence of the PLA to ENR ratio in thermoplastic vulcanizate (TPV) and the impact of the addition of double-decker silsesquioxanes functionalized with four 2-(2-ethoxy)ethanol groups (DDSQ-eter-4OH) to TPV. Effects on the mechanical and thermal properties, apparent cross-linking density, and thermo-oxidative stability of the PLA/ENR blends prepared via the dynamic vulcanization method were also

examined. To assess the degree of association of DDSQ-eter-4OH with the remaining TPV components, extraction in dichloromethane was performed to wash out the unbound PLA, and then Fourier infrared spectroscopy (FTIR) examination of the samples before and after extraction was performed.

EXPERIMENTAL PART

Materials

The following materials have been used in this study: polylactide (PLA) with 95.8% LLA content and a molecular weight of 113,000 g/mol, produced under the trade name Ingeo 4043D, (Nature Works, Minnetonka, USA); epoxidized natural rubber (Epoxyprene 50) was provided by Resinex UK (Mooney viscosity: 70–100 and epoxidation = 50 ± 2). DDSQ-eter-4OH was used as the compatibilizer which structure is presented in Figure 1. The compound was obtained according to the known hydrosilylation protocol of tetrahydrofunctional double-decker silsesquioxanes and 2-(vinyloxy)ethanol in the presence of Pt-Karstedt catalyst with 95% yield, depicted in Scheme 1 [51]. Norperox DPC-40 dicumyl peroxide (Nordmann AT Group, Vienna, Austria) was used as a cross-linking agent and Irganox 1010 (Basf, Ludwigshafen am Rhein, Germany) as an antioxidant.

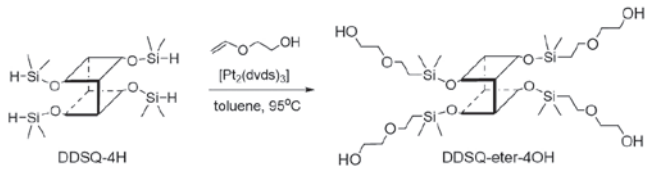

Scheme 1. Synthesis of DDSQ-eter-4OH

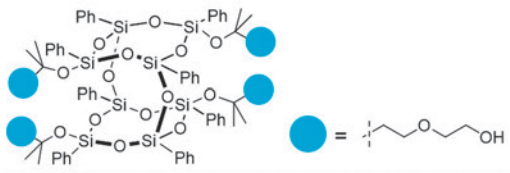

Fig. 1. Structure of double-decker silsesquioxane (DDSQ-eter-4OH)

Dynamic vulcanization

PLA/ENR vulcanizates were prepared by dynamic vulcanization in a Brabender Plastograph (Duisburg, Germany), which allows for mixing at elevated temperatures. Before compounding, PLA was dried in a vacuum at 80°C for 24 hours. Six mixtures were prepared: four with the PLA/ENR wt ratio of 90/10, 80/20, 70/30, and 60/40; and two mixtures with PLA/ENR ratio of 60/40 containing 2.5 wt% and 5 wt% of DDSQ-eter-4OH. Dicumyl peroxide was used as a cross-linking agent in an amount of 1.5 wt% in relation to ENR, and Irganox 1010 was used as an antioxidant in an amount of 0.2 wt%. Dynamic vulcanization was conducted at a temperature of 155°C. The kneader rotation during the processing was 40 rpm. In the first stage, neat PLA was plasticized. After approximately 3 minutes, Irganox 1010 was incorporated and mixed for another 2 minutes until the antioxidant was thoroughly distributed in the molten PLA. Then, a small amount of ground ENR rubber was gradually added to form a homogeneous mixture with PLA. After achieving this effect, the mixing process continued for about 5 minutes. In the case of samples containing DDSQ-eter-4OH, it was right after adding the rubber into the system and subsequently mixing for another 5 minutes to distribute the DDSQ-eter-4OH throughout the mixture. Once this effect was achieved, dicumyl peroxide was added, and the mixing process was continued for another 5 minutes. After processing, the obtained thermoplastic vulcanizate was removed from the mixing chamber.

Pressing of thermoplastic vulcanizates

The obtained thermoplastic vulcanizates were pressed in a Planet Press P 200 E hydraulic press (Dr Collin GmbH, Germany) at temperature of 160°C with pressure of approx. 10 MPa for 5 minutes. In this way, samples were obtained in the form of thin plates with an optically homogeneous structure. The plates were cut into smaller fragments that could be subjected to the injection process.

Preparation of testing samples

The testing samples, type A3 according to EN ISO 527-2 (Figure 2) were injection molded using Boy 15 injection molding machine (Dr Boy GmbH&Co., Neustadt, Germany). The parameters of injection molding were as follows: the temperatures of the plasticizing zones (in order from the hopper) were: 170°C, 200°C and 210°C, respectively; the injection pressure was 100 MPa, and the holding pressure was 35 MPa. The cooling time for the molded parts was 30 s.

Thermal aging

To study the impact of the aging process on the mechanical properties of neat PLA and PLA/ENR vulcanizates, they were subjected to a thermal aging. The process was conducted in an oven at 70°C for 168 hours (7 days) without vacuum. Samples subjected to the aging process are marked with the index "S".

Preparation of samples for apparent cross-linking density testing in toluene

Specimens for evaluating the cross-linking density in toluene were cut from previously injection-molded parts.

These samples were rectangular plates with dimensions of 7 × 7 × 2 mm.

Preparation of samples for FTIR spectroscopy by PLA extraction

To remove the unbound PLA from the vulcanizates, the obtained materials were subjected to an extraction process. Extraction was performed in dichloromethane at 40°C for 72 hours (3 days). The exact mass of samples before extraction (ca. 4 g), the mass of empty thimbles used for extraction, and the mass of thimbles with contents before and after extraction were measured. Samples after extraction in dichloromethane were marked with the letter "E".

Methods

Tensile properties

The tensile properties of neat PLA and thermoplastic vulcanizates before and after the aging process were measured according to PN-EN ISO 527 and PN-EN ISO 178 using an Autograph AG-X plus tensile testing machine (Shimadzu, Kyoto, Japan) equipped with 1 kN load cell, a contact optical long-travel extensometer and the Trapezium X computer software (Shimadzu, Kyoto, Japan), operated at a constant crosshead speed of 5 mm/min. Measurements were performed at room temperature on the paddle-shaped samples (type A3) with a grip distance of 20 mm. The Young's modulus, tensile strength (σ_y) and elongation at yield (ε_y), strength at break (σ_b) and elongation at break (ε_b) of the vulcanizates were determined. Seven measurements were conducted for each sample, and the results were averaged to obtain a mean value.

Shore hardness

The hardness was investigated according to PN-EN ISO 868 using a Zwick 3100 Shore A tester (Zwick GmbH, Ulm, Germany). The reported values were the average of 10 independent measurements.

Hydrostatic density

The hydrostatic density was evaluated using the Radwag AS 160/C/2 scale (Radom, Poland) in distilled water at 22°C. At least 10 measurements were made for each material, and the mean and standard deviation were determined.

Differential scanning calorimetry

Differential scanning calorimetry (DSC) was performed at a heating rate of 10°C/min, in nitrogen atmosphere (20 ml/min), with a scan range of temperature from -85°C to 200°C in a heating/cooling/heating cycle using DSC 204 F1 Phoenix apparatus (Netzsch, Selb, Germany). The tested samples (10 ± 0.5 mg) were placed in separate aluminum pans. The characteristic phase transition temperatures (glass transition and melting) were taken from the second heating run. Glass transition temperature (T_g) was determined using the midpoint approach, while specific heat capacity (ΔC_p) was calculated from the vertical distance between extrapolated baselines at T_g. The crystallization (T_c) and melting (T_m) temperatures were determined from the maximum of the exothermic and endothermic peaks, respectively. The heat of fusion (ΔH_m) and crystallization (ΔH_c) were calculated from the total areas under melting and crystallization peaks on the DSC curves.

Thermo-oxidative stability

The thermo-oxidative stability of PLA and PLA/ENR were evaluated using TGA 92-16.18 thermobalance (Setaram, Caluire-et-Cuire, France). Measurements were conducted at dry synthetic air (N_2:O_2 = 80:20 vol. %) at a flow rate of 20 mL/min. The study was conducted at a heating rate of 10°C/min in the temperature range of 20–700°C. Measurements were conducted following the PN-EN ISO 11358 standard.

FTIR analysis

Attenuated total reflectance – Fourier transform infrared (ATR-FTIR) spectra of PLA and PLA/ENR were recorded using FTIR spectrophotometer Tensor 27 (Bruker Optic GmbH, Billerica, MA, USA). Measurements were taken with 32 scans and a resolution of 2 cm^{-1} over the wavenumber range of 4000–400 cm^{-1}. The comparative analysis of the functional groups presents in the considered samples, using infrared spectroscopy (FTIR), became the basis for assessing the type of material and confirmed the presence of characteristic functional groups appropriate for the position of the transmission spectrum waves of the ENR- and POSS-modified polylactide groups.

Cross-linking density

The apparent cross-linking density was evaluated for each of the thermoplastic vulcanizates by placing previously cut samples with dimensions of 7 × 7 × 2 mm in toluene 20°C. The mass of the samples was measured before they were placed in toluene, and after immersion for 1, 2, 3, 4, 24, 48, and 72 hours (after reaching the swelling equilibrium). Before measuring the mass, each sample was thoroughly wiped of toluene with a lint-free towel. Photos of the samples after reaching the swelling equilibrium are shown in Figure 2. The cross-linking density was calculated using Eq. 1 [52]. The density calculated in this way is a dimensionless value.

$$V_r = \frac{1}{1+\left(\frac{m_1}{m_2}-1\right)\cdot\frac{\varrho_k}{\lambda\cdot\varrho_t}} \quad (1)$$

where: V_r – apparent cross-linking density, m_1 – mass of the sample before reaching the swelling equilibrium state, m_2 – sample mass after reaching the swelling equilibrium state, ϱ_t – toluene density (0.865 g/cm^3), ϱ_k – ENR density (1.25 g/cm^3), λ – ENR mass content in the thermoplastic vulcanizate.

Fig. 2. Samples after reaching the swelling equilibrium state, from left: PLA/ENR vulcanizates: 90/10, 80/20, 70/30, 60/40, 60/40_ DDSQ-eter-4OH, 60/40_ DDSQ-eter-4OH _5

RESULTS AND DISCUSSION

Mechanical properties

By comparing the stress-strain curves obtained during the static tensile test (Figure 3) and the values of tensile moduli, as well as the stress and elongation values listed in Table 1, a significant impact of ENR on PLA mechanical performance can be found. In both cases of unaged and aged samples, a decrease in the tensile stress, stress at break, and an increase in the elongation at yield mean values of the samples are observed with an increase in the content of ENR in the TPVs. Both neat PLA and samples containing 19% ENR cracked immediately after reaching the yield point, without achieving elongations above 5%, revealing typical brittle behavior. Only the addition of ENR in the amount of 20 wt% and more allowed for higher elongations to be achieved, but at the expense of lowering the maximum recorded stresses in the material. However, the highest elongations, both in the case of unaged and aged samples, were noted for samples with an ENR content of 30% (253.9% ± 3.2 for the unaged sample and 208.7% ± 17.4 for the aged sample). Adding ENR to the vulcanizate in larger amounts (40%) caused another reduction in the elongation at the break value. Each of the tested samples achieved a similar value of elongation at yield. In each case, the value of ε_y was approximately 2–3%. The addition of DDSQ-eter-4OH in amounts of 2.5 and 5 wt% also had a noticeable effect on the mechanical properties of the samples. As the amount of DDSQ-eter-4OH increased, a significant decrease in the value of elongation at break was observed. Similar observations on the deteriorated effect of POSS particles on the tensile strength and elongation at break were observed by Jeziórska *et al.* [53]. Our studies are also in agreement with the ones made by Lipińska *et al.* [54], who also prepared PLA/ENR blends, but glycidyl-POSS and trisilanolisooctyl-POSS were used as functional additives. They observed the reinforcing effect of the incorporation of PLA in the PLA/ENR blend. The higher the ENR content in the blend, the lower the elongation at break noticed. The formation of covalent bonds between PLA and ENR phases reduced the elasticity of the blend, at the same time, the system's strength was enhanced. Substantial reduction of the elongation at break ε_b after the modification of 40:60 PLA/ENR by Gly-POSS was observed

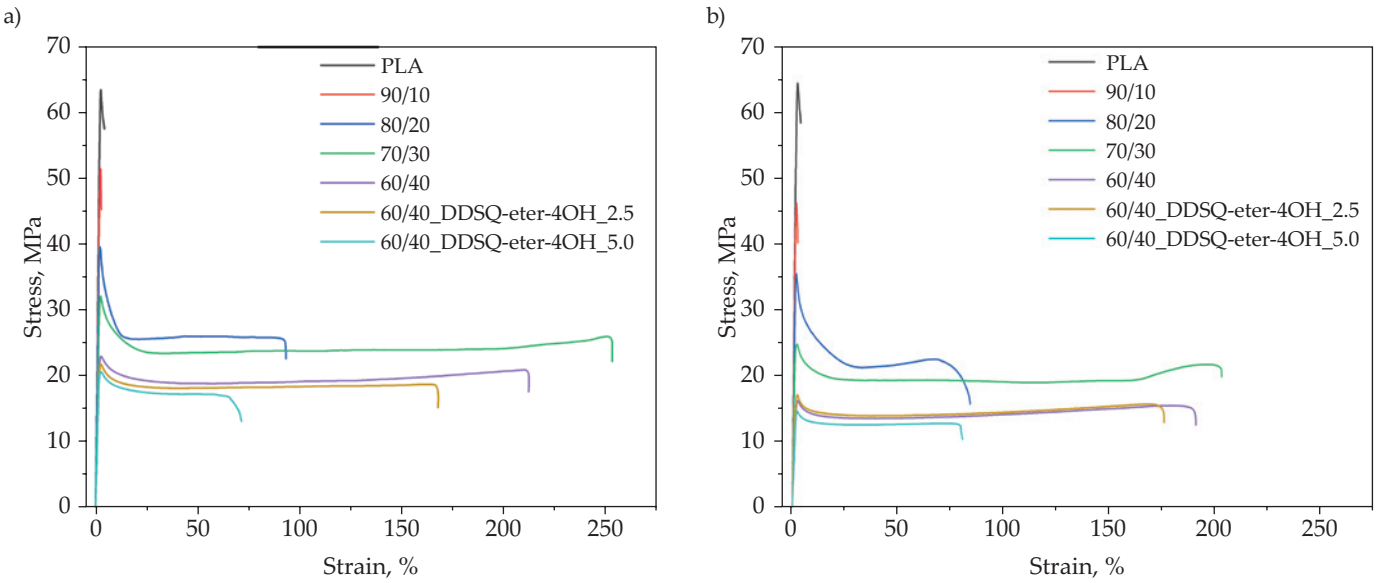

Fig. 3. Stress-strain curves of PLA and PLA/ENR vulcanizates: a) before aging, b) after aging

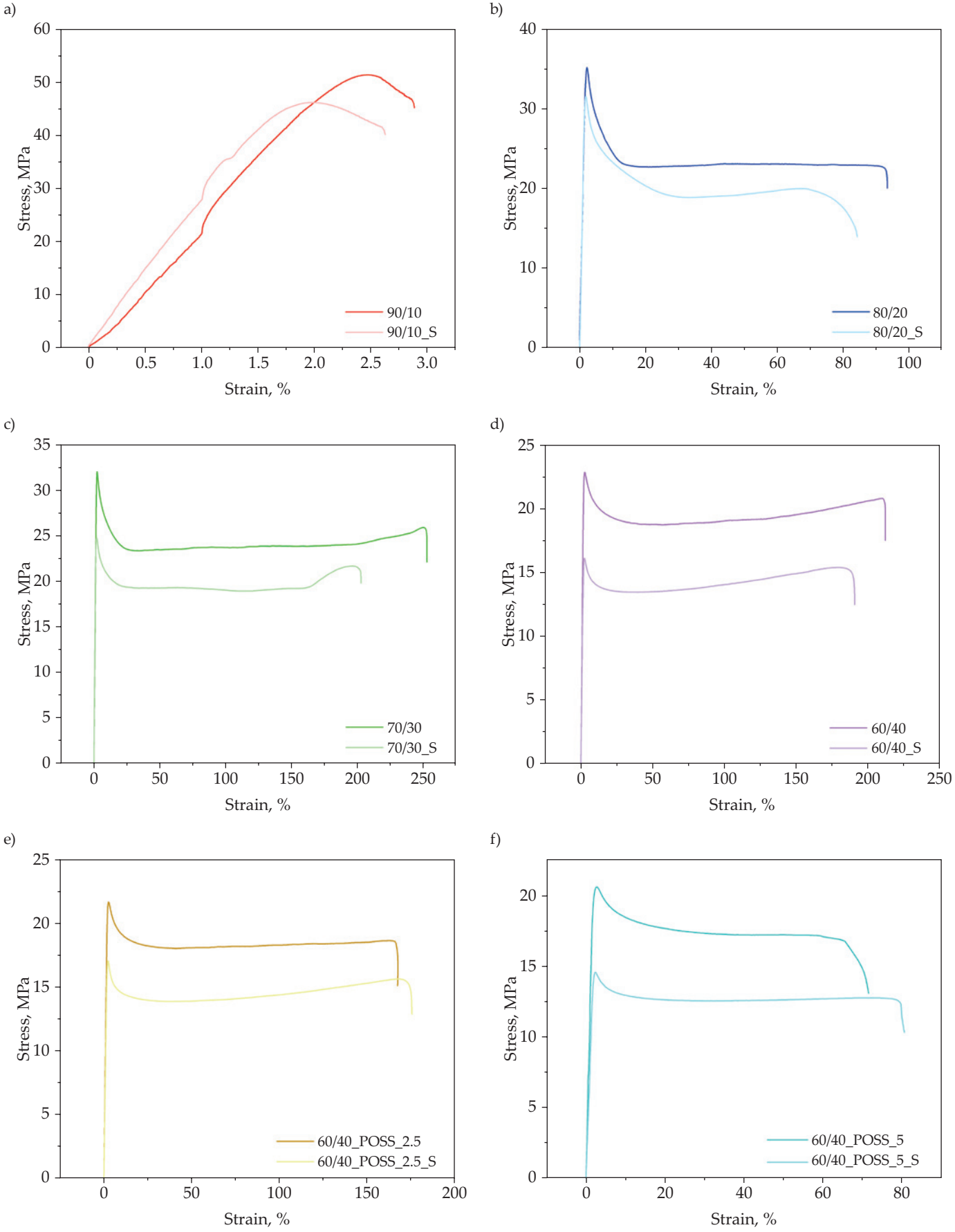

Fig. 4. Stress-strain curves of PLA/ENR vulcanizates before and after aging

along with lower values of tensile strength as compared with the blend modified by HO-POSS. They explained that this effect can result from the higher cross-link density of the blend. OV-POSS could have functioned as a multifunctional cross-link reducing the material's elasticity. At the same time, additional cross-links caused excessive brittleness of the material and decreased TS values.

The stress-strain curves of the aged samples are shown in Figure 4, and the characteristic values are summarized in Table 1. After the aging process, the strength properties of the samples, and particularly the tensile stress, slightly deteriorated. The deterioration of properties occurred in proportion to the content of the elastomeric component in thermoplastic vulcanizates. The higher the content of ENR in the sample, the lower the values of stress at the yield and stress at break were recorded. The elongations at break did not change significantly after aging. Only after the incorporation of DDSQ-eter-4OH a slight decrease was vis visible. This difference is clearly visible between samples with 2.5 and 5 wt% of DDSQ-eter-4OH (especially in the case of aged samples). It is possible that the reduction in maximum elongations is due to the increase in the degree of ENR cross-linking in these samples, which may have been influenced by the addition of DDSQ-eter-4OH. The tensile stress achieved during the tensile test did not change significantly after the introduction of DDSQ-eter-4OH.

According to the conducted research, the addition of DDSQ-eter-4OH affects the aging process of materials, which can be observed in Figure 4. As a result of the increased temperature, the values of elongation at break of the aged samples increased slightly. However, in the case of unaged materials containing DDSQ-eter-4OH, the elongation at break is much lower, but the strength remains almost unchanged, which may indicate the influence of the additive on the cross-linking process and the formation of a larger number of bonds connecting the PLA with ENR [27, 54, 55].

The results of hardness measurements of the tested samples are presented in Table 1. As the tests show, the hardness of TPV decreases with the increasing amount of ENR. Adding 40% ENR to PLA resulted in a decrease in the ShA value by 15, which means a change of as much as 23%. This is quite a significant result. In addition, as expected, after aging, one could have observed an increase in hardness of about 30 to even 60%. The increase in hardness after aging can be attributed to several factors related to the molecular and structural changes that occur over time, crystallization (increase crystallinity) and crosslinking (formation of covalent bonds). In turn, the negligible effect of the silsesquioxanes addition on hardness is caused by the dominant share of the elastic phase in the blend and the lack of reinforcing effect of the nanostructured additive. The second mechanism that may cause an increase in the hardness of PLA is changes in its crystalline structure [56]. However, considering the used in this study, PLA grade with a low tendency to crystallize from the melt and the low tendency of POSS to heterogeneous nucleation [57], the observed results are reasonable. Similarly, Dandan Doganci [58] did not observe a beneficial improvement in hardness caused by the presence of nanostructured domains in the PLA-based blend when producing PLA from POSS cored star poly(ε-caprolactone).

Table 1 also shows the values of hydrostatic densities of samples. As expected, samples with a higher ENR content

T a b l e 1. Mechanical properties of PLA and PLA/ENR vulcanizates before and after aging

Sample	E, MPa	σ_y, MPa	ε_y, %	σ_b, MPa	ε_b, %	H, Sh°A	d, g/cm^3
Before aging							
PLA	2324±238	64.13±0.76	2.48±0.19	63.47±0.82	4.5±1.2	66.0±1.0	1.243
90/10	2213±101	50.34±1.01	2.30±0.07	51.45±1.12	1.7±0.9	65.1±1.0	1.214
80/20	1844±107	39.28±0.33	2.30±0.04	25.62±0.56	87.5±5.0	61.5±1.0	1.182
70/30	1312±75	32.10±0.23	2.63±0.12	23.94±0.38	253.9±3.2	60.4±1.0	1.155
60/40	952±23	22.77±0.20	2.86±0.07	20.89±0.29	211.2±1.6	51.4±1.0	1.136
60/40_ DDSQ-eter-4OH_2,5	954±81	21.78±0.14	2.63±0.06	18.62±0.21	129.2±9.8	51.2±1.0	1.135
60/40_ DDSQ-eter-4OH_5	936±153	20.65±0.07	2.86±0.03	16.83±0.11	68.0±6.3	51.0±1.0	1.132
After aging							
PLA	3050±192	64.31±0.17	2.72±0.15	63.45±0.31	3.5±0.2	93±1.0	1.715
90/10	2757±236	46.45±0.73	2.70±0.38	46.24±0.97	3.5±5.6	94±1.0	1.712
80/20	2054±240	34.92±0.40	2.45±0.49	22.49±0.68	136.5±17.4	91±1.0	1.643
70/30	1794±16	25.35±0.48	1.90±0.35	21.28±0.63	208.7±17.4	88±1.0	1.582
60/40	956±48	17.21±0.48	2.27±0.18	15.22±0.59	155.5±29.0	82±1.0	1.151
60/40_ DDSQ-eter-4OH_2,5	684±17	16.29±0.30	3.01±0.35	15.62±0.51	171.0±15.7	77±1.0	1.510
60/40_ DDSQ-eter-4OH_5	647±5	13.01±0.19	2.68±0.24	12.54±0.14	82.5±13.0	75±1.0	1.498

E – Young's modulus; σ_y, ε_y – tensile strength and elongation at yield, respectively; σ_b, ε_b – tensile strength and elongation at break, respectively; H – shore hardness; d – hydrostatic density

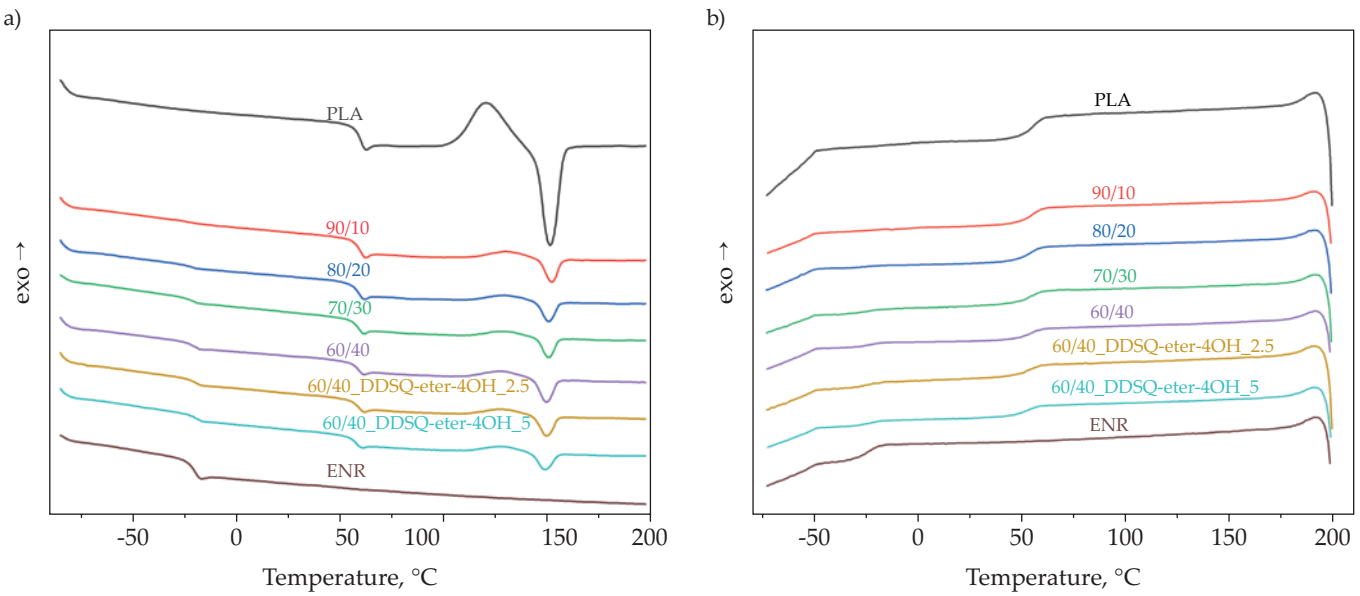

Fig. 5. DSC thermograms of PLA and PLA/ENR vulcanizates: a) the second heating, b) cooling

showed lower density than samples with a higher PLA content. This is since neat PLA has a higher density than ENR. The addition of POSS to thermoplastic vulcanizates with an ENR content of 40% did not significantly affect their density. Maintaining a linear relationship with the density change also proves the correct preparation of the composition and the proper uniformity of the blends. The influence of the aging process on the increase in hydrostatic density values was also observed. The increase in the hydrostatic density value after aging is also dictated by molecular and structural changes in the materials, i.e., higher crystallinity and formation of additional chemical bonds (cross-links) between polymer chains.

Thermal properties

The DSC thermograms recorded during the second heating and cooling are presented in Figure 5. The characteristic phase transition temperatures and the corresponding enthalpies of these phase transitions are presented in Table 2. Based on the second heating (Figure 5a), one can assume that both ENR and PLA demonstrate an amorphous nature. For neat PLA and all TPVs, cold crystallization exotherms and melting peaks can be detected in the second heating scans. In turn, none of the tested materials exhibited crystallization from the molten state (cooling thermograms, Figure 5b).

All vulcanizates, except for the system containing 90% PLA, showed two glass transitions. With the increase in the amount of ENR in the system, a shift of the T_{g2} value (from PLA) towards lower temperatures (plasticizing effect) was observed, and the glass transition associated with ENR was identical for all TPVs. Only the addition of DDSQ-eter-4OH caused a slight shift of the T_{g1} value towards higher temperatures. Moreover, the ΔC_{p1} values, as expected, increase with the increase in the content of ENR in the TPVs.

By analyzing the values of melting temperatures for vulcanizates and comparing them to the neat PLA, slight reduction in the value of T_m along with a significant reduc-

T a b l e 2. Thermal properties of PLA and PLA/ENR vulcanizates determined from DSC

Sample	Glass transition				Cold crystallization		Melting	
	T_{g1}, °C	ΔC_{p1}, J/g · °C	T_{g2}, °C	ΔC_{p2}, J/g · °C	T_{cc}, °C	ΔH_{cc}, J/g	T_m, °C	ΔH_m, J/g
PLA	–	–	58.7	0.656	120.1	25.26	151.2	26.86
90/10	–	–	58.4	0.429	129.2	3.979	152.0	4.75
80/20	-21.2	0.092	57.6	0.415	129.2	3.428	150.8	4.197
70/30	-21.2	0.146	57.6	0.347	127.6	3.010	150.4	3.966
60/40	-21.1	0.179	56.5	0.624	127.,5	2.028	149.3	5.151
60/40_ DDSQ-eter-4OH_2,5	-19.7	0.151	58.5	0.288	126.3	4.876	149.7	5.081
60/40_ DDSQ-eter-4OH_5	-19.6	0.148	57.1	0.257	127.8	4.52	149.0	5.466
ENR	-21.2	0.499	–	–	–	–	–	–

T_{g1}, T_{g2} – glass transition temperature of ENR and PLA respectively; ΔC_{p1}, ΔC_{p2} – change of heat capacity at T_{g1}, T_{g2} respectively; T_{cc}, ΔH_{cc} – temperature and enthalpy of cold crystallization); T_m, ΔH_m – temperature and enthalpy of melting

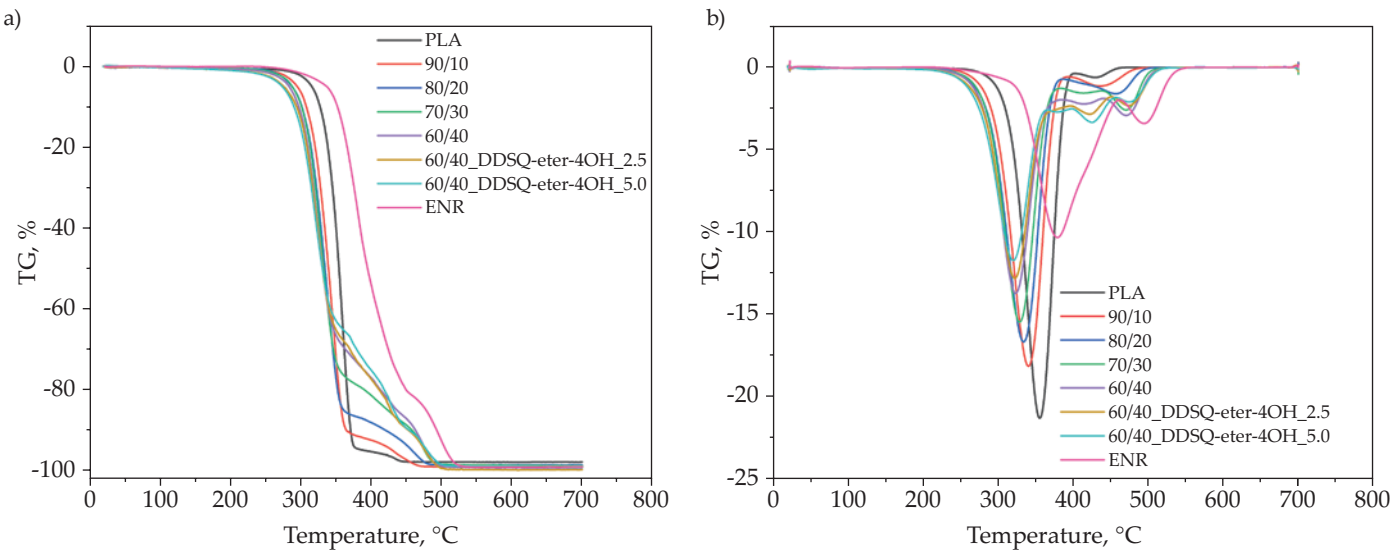

Fig. 6. Curves of PLA and PLA/ENR vulcanizates: a) TG, b) DTG

T a b l e 3. TGA data of PLA and PLA/ENR vulcanizates

Sample	$T_{5\%}$ °C	T_{DTG1} PLA °C	T_{DTG2} PLA °C	T_{DTG3} ENR °C	T_{DTG4} ENR °C
PLA	316	355	425	–	–
90/10	295	340	436	–	–
80/20	288	334	457	–	–
70/30	287	328	–	413	471
60/40	283	323	–	415	471
60/40_ DDSQ-eter-4OH_2,5	276	322	–	423	474
60/40_ DDSQ-eter-4OH_5	276	320	–	425	475
ENR	337	–	–	379	394

tion in the values of enthalpies of cold crystallization (ΔH_{cc}) and melting (ΔH_m) can be observed. Moreover, the incorporation of ENR into PLA caused firstly an increase in the value of T_{cc} and, subsequently, its further decrease along with the increase in ENR content in TPVs.

It can, therefore, be concluded that the incorporation of DDSQ-eter-4OH limited the molecular mobility around the glass transition temperature [59]. This effect may be caused by the increase in cross-linking of the ENR chains because of the introduction of additional reactive groups with the compatibilizer, which may indicate its incorporation into the structure of cross-linked rubber [41, 42, 54].

TGA analysis of the samples allowed for the assessment of the thermal decomposition rate of the samples (mass loss) with increasing temperature (Figure 6). In addition, the temperature of the 5% mass loss, as well as the temperatures corresponding to the maximum mass losses (T_{DTG1}, T_{DTG2}, T_{DTG3}, T_{DTG4}), can be found in Table 4. Among the tested materials, the highest value of $T_{5\%}$ value was recorded for neat PLA ($T_{5\%}$ = 315°C) and for neat ENR ($T_{5\%}$ = 337°C). The $T_{5\%}$ temperatures of the tested vulcanizates were noticeably lower compared to the reference samples. Moreover, as the content of ENR in the vulcanizate increased, the value of $T_{5\%}$ decreased. In the case of vulcanizates containing DDSQ-eter-4OH, the $T_{5\%}$ temperature was the lowest, and the percentage of DDSQ-eter-4OH did not affect its value. For both vulcanizates containing 2.5 and 5 wt% DDSQ-eter-4OH, this temperature was comparable (276°C and 276°C, respectively).

To better present the corresponding thermal degradation peak, DTG curves were presented in Figure 6b). Neat PLA and ENR showed double thermal degradation peaks (355°C and 423°C for PLA, 378°C and 394°C for ENR). Vulcanizates with lower amounts of ENR (10 and 20%) showed two thermal degradation peaks, first close to PLA, and second close to ENR, which demonstrated that part of PLA was grafted on ENR network (PLA-g-ENR). However, the degradation peak temperature of the PLA phase in the vulcanized part of TPV was lower than neat PLA. This was due to the grafted PLA resulting from dynamic vulcanization processing [55]. More complicated DTG curves was obtained for the TPVs with more than 20% of ENR, *i.e.*, 30 and 40%, and samples containing DDSQ-eter-4OH. Here, three degradation peaks were observed - first, the most intense, close to PLA, and

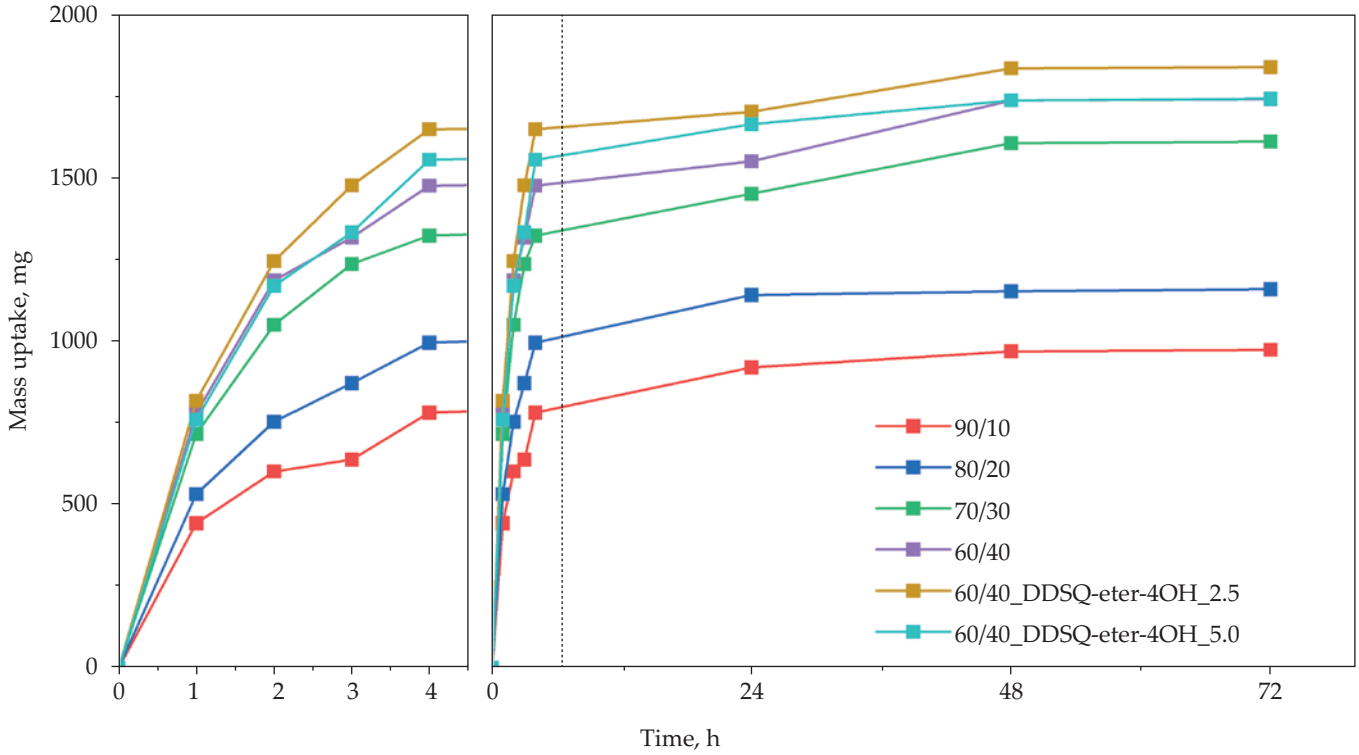

Fig. 7. Mass uptake over time of PLA/ENR vulcanizates immersed in toluene

the other two, close to ENR. Moreover, the degradation peak temperature of the ENR phase in the vulcanized part of TPV was higher than neat ENR, which may be attributed to PLA grafting on the surface of the ENR network to delay ENR degradation.

It is worth noting that introducing DDSQ-eter-4OH in the vulcanizate containing 40% ENR also resulted in a shift of the T_{DTG} peak for ENR towards higher values. This may prove the grafting of DDSQ-eter-4OH into the ENR structure, as the degradation of ENR occurred later in vulcanizates containing DDSQ-eter-4OH compared to vulcanizates with the same PLA to ENR ratio but without the addition of DDSQ-eter-4OH. This indicates that DDSQ-eter-4OH can play the role of radical trap via consuming the highly reactive hydrogen and hydroxyl radicals so that they increase the onset degradation temperature of the ENR [35, 60].

Absorption and apparent cross-linking density

Figure 7 shows the mass intake of samples immersed in toluene. Mass measurements were taken during the first 4 hours of the study and every 24 hours for the next 3 days. Analyzing the course of the graph during the first 4 hours of the test, it can be clearly observed that samples with a higher ENR content absorbed toluene much faster, and their mass intakes increased in a stronger manner. It is also worth noting that samples containing 2.5 and 5 wt% DDSQ-eter-4OH also absorbed slightly faster than the reference (60/40), but only in the case of the sample with 5 wt% of DDSQ-eter-4OH the final mass intake was greater. Samples with 10 and 20 of ENR content reached the after approximately 24 hours. After this time, the mass intakes were minimal. The remaining samples reached the swelling equilibrium state after approximately 48 hours.

Table 4 shows the apparent cross-linking density of the tested samples calculated according to Eq. 1. Analyzing the results, an increase in the cross-linking density of the vulcanizate is observed with an increase in the ENR share up to 30%. In turn, the higher amount of ENR in the vulcanizate caused the apparent cross-linking density value to decrease. At the same time, it was found that in the system of 60/40, the incorporation of DDSQ-eter-4OH did not noticeably affect the cross-linking density. Such an increase in the apparent cross-linking density for the vulcanizate with an ENR content of not more than 30% might refer to the greater number of cross-links or chemical bonds formed between polymer chains within the analyzed material. Further increasing the amount of ENR in

T a b l e 4. The apparent cross-linking density of PLA/ENR vulcanizates

Sample	Apparent cross-linking density, g/cm^3
90/10	0.860
80/20	0.905
70/30	0.933
60/40	0.915
60/40_ DDSQ-eter-4OH_2,5	0.916
60/40_ DDSQ-eter-4OH_5	0.913

the system has led to a change in the structural character of this composition. Thus, increasing the amount of ENR in the analyzed vulcanizates to 40% leads to phase inversion, and the matrix (PLA) turns into the dispersed phase, while ENR takes over the role of the dominant phase.

FTIR analysis

The FTIR analysis was performed to examine the chemical structure of physical blends. The obtained spectra for neat materials and blends without further modification are presented in Figure 8. Additionally, spectra for materials after extraction in dichloromethane and with POSS content are presented in Figure 10. The peaks at 1080 cm^{-1} and 1184 cm^{-1} visible for neat PLA and blends can be ascribed to C-O-C stretching [5, 61, 62]. The sharp peak at 1749 cm^{-1} is typical for stretching ester carbonyl C=O groups [63]. Furthermore, for every material, one can observe -CH_3 symmetrical and asymmetrical bending at 1361 cm^{-1} and 1452 cm^{-1}, respectively [61, 64, 65]. Moreover, the C-H stretching vibrations have been identified at 2820–2995 cm^{-1} [5, 64]. The characteristic peak for ENR at 1249 cm^{-1} is assigned for the symmetrical stretching vibration of the epoxy ring [64]. The peaks corresponding to the asymmetrical stretching vibration of the epoxy ring can be found at 875 cm^{-1} and 832 cm^{-1} [66, 67]. With the increasing content of ENR, the peaks associated with vibration are more visible due to higher intensity. Furthermore, peaks related to C-H stretching vibrations, as well as symmetrical and asymmetrical bending, become more visible with higher ENR content.

By analyzing the FTIR spectra for samples 70/30 and 60/40 before and after extraction (Figure 9), it can be concluded that some of the PLA macromolecules were attached to the ENR chains during dynamic vulcanization. After extraction in dichloromethane, the PLA that did not produce bond to ENR was washed out, as evidenced by a decrease in the intensity of the spectrum at wavelengths of 1750 cm^{-1}, 1184 cm^{-1}, and 1080 cm^{-1} and a slight increase in intensity at a wavelength of 1370 cm^{-1}. Additionally, the peak at the wavenumber of 1750 cm^{-1} (responsible for the stretching vibrations of the C=O groups present in PLA) was shifted to the wave number of 1755 cm^{-1}, which may indicate a chemical interaction between PLA and ENR. The probable mechanism of combining PLA macromolecules with ENR is based on the initiation of active points (e.g., without tertiary carbon) on PLA macromolecules by hydrogen atoms originating from dicumyl peroxide-containing radicals. These points were able to react with ENR chains (or ENR radicals) to form a PLA-g-ENR graft copolymer at the PLA-ENR interface, binding part of the PLA dispersed phase. Moreover, when comparing the series of vulcanizates with the addition of DDSQ-eter-4OH before and after extraction, a noticeable decrease in intensity is observed at the wavenumber of 1750 cm^{-1} for the extracted samples (responsible for the stretching vibrations of the C=O groups present in PLA). However, this peak is evident enough even after extracting unbound PLA from the samples. This allows us to assume that the DDSQ-eter-4OH present in vulcanizates helped bind PLA to ENR, so that even after extraction, the peak at the wave number of 1750 cm^{-1} is visible.

CONCLUSIONS

The selected properties of thermoplastic vulcanizates based on polylactide and epoxidized natural rubber were examined. The incorporation of ENR into the PLA structure was clearly demonstrated, as well as the influence of the addition of DDSQ-eter-4OH on the properties of the system (FTIR). Moreover, FTIR examination of thermoplastic vulcanizates extracted in dichloromethane seems

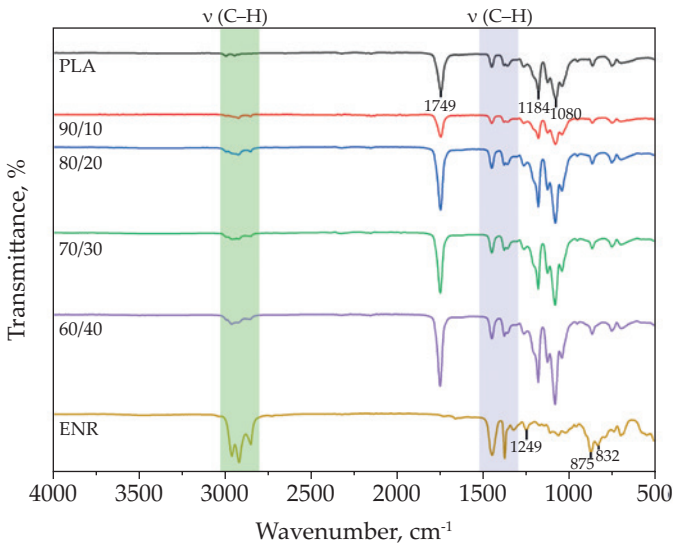

Fig. 8. The FTIR spectra of PLA and PLA/ENR vulcanizates

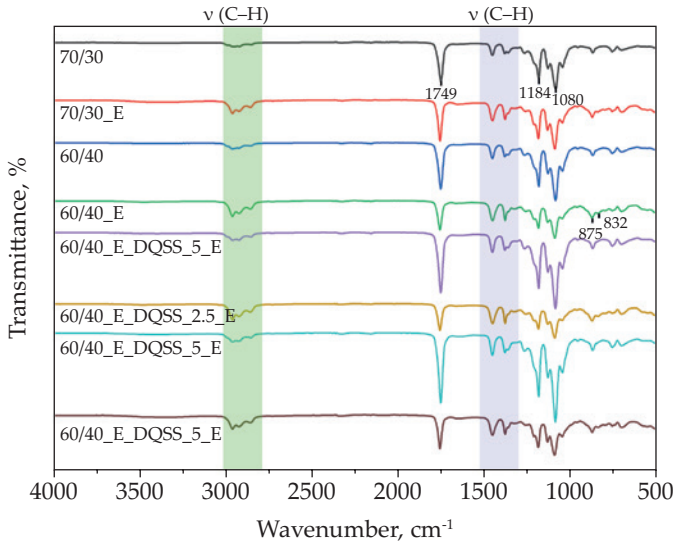

Fig. 9. The FTIR spectra of PLA/ENR vulcanizates after extraction in dichloromethane and with addition of DDSQ-eter-4OH

to confirm the chemical bonding of PLA and ENR at the phase boundary: formation of macromolecules of the PLA-g-ENR copolymer. Moreover, the analysis of the FTIR spectrum of the extracted sample with 5 wt.% DDSQ-eter-4OH showed a greater bonding degree between PLA and ENR, which clearly confirms the compatibilizing effect of DDSQ-eter-4OH. It was also shown that the incorporation of 10 wt% of ENR resulted in a distinct change in mechanical properties. Samples containing a smaller amount of rubber show mechanical properties typical of brittle and stiff materials (high maximum stress and low elongation at break), which was predictable due to the brittle nature of neat PLA. However, as the rubber content increased, the samples began to show characteristics more like elastomeric materials - the elongation at break increased at the expense of the maximum stress, which proves that ENR was incorporated into the PLA structure. The greatest improvement in elongation at break was observed with TPV containing 30 wt% ENR. However, a higher ENR content (40 wt%) resulted in lowering the value of elongation at break. By analyzing the stress-strain curves, conclusions can also be drawn regarding the effect of the DDSQ-eter-4OH addition on the properties. Samples containing DDSQ-eter-4OH showed a significant reduction in maximum elongation while maintaining the same maximum stress as samples without DDSQ-eter-4OH. This allows us to assume that DDSQ-eter-4OH was incorporated into the structure of vulcanizates, thus increasing the degree of cross-linking and stiffening the material. Aging resulted in the deterioration of all mechanical properties. In the case of PLA/ENR without DDSQ-eter-4OH, both the maximum stress and the elongation at break were reduced. However, it is worth noting that in the case of PLA/ENR containing both 2.5 and 5 wt% DDSQ-eter-4OH, the elongation at break increased after samples' aging.

By analyzing DSC thermograms, the amorphous nature of the PLA/ENR vulcanizates was demonstrated. The addition of DDSQ-eter-4OH resulted in a slight reduction in the glass transition temperature from ENR. At the same time, the analysis of TG curves showed a shift in the temperature value of 5% mass loss with an increase in ENR content, and in the system containing DDSQ-eter-4OH an increase in thermal stability was observed. This may confirm the incorporation of DDSQ-eter-4OH into the ENR and the increase in cross-linking of this structure.

The analyzed PLA/ENR systems, especially those compatibilized with silsesquioxanes can be used in various fields, especially where the properties of both PLA and ENR are required. Here are some areas where such systems can be used: i) in the production of flexible food packaging; ii) for the production of foils and bags, iii) for the production of household products, such as flexible covers or mats; iv) in the sports industry for the production of flexible elements, such as soles for sports shoes, armbands or protectors, v) for the production of flexible insulating materials that can be used in the electrical or construction industry; vi) for 3D printing, enabling the creation of flexible and durable models, vii) in the production of gaskets, sealants or flexible edges and viii) for the production of flexible components such as seals or shock absorption elements in the automotive industry. The above applications show that systems based on PLA with epoxidized natural rubber can be used in various fields, combining the advantages of both materials, and meeting the specific requirements of a given application.

REFERENCES

[1] Rasal R.M., Janorkar A. V., Hirt D.E.: *Progress in Polymer Science* **2010**, *35(3)*, 338. https://doi.org/10.1016/j.progpolymsci.2009.12.003

[2] Bogaert J.-C., Coszach P.: *Macromolecular Symposia* **2000**, *153(1)*, 287. https://doi.org/10.1002/1521-3900(200003)153:1<287:aid-masy287>3.0.co;2-e

[3] Theryo G., Jing F., Pitet L.M. *et al*.: *Macromolecules* **2010**, *43*, 7394. https://doi.org/10.1021/ma101155p

[4] Grijpma D.W., Nijenhuis A.J., Van Wijk P.G.T. *et al*.: *Polymer Bulletin* **1992**, *29*, 571. https://doi.org/10.1007/BF00296720

[5] Irska I., Paszkiewicz S., Gorący K. *et al*.: *Express Polymer Letters* **2020**, *14*, 26. https://doi.org/10.3144/expresspolymlett.2020.4

[6] Murariu M., Da Silva Ferreira A., Alexandre M. *et al*.: *Polymers for Advanced Technologies* **2008**, *19(6)*, 636. https://doi.org/10.1002/pat.1131

[7] Lemmouchi Y., Murariu M., Santos A.M.D. *et al*.: *European Polymer Journal* **2009**, *45(10)*, 2839. https://doi.org/10.1016/j.eurpolymj.2009.07.006

[8] Przybysz-Romatowska M., Barczewski M., Mania S. *et al*.: *Materials* **2021**, *14(15)*, 4205. https://doi.org/10.3390/ma14154205

[9] Anderson K.S., Hillmyer M.A.: *Polymer (Guildf)* **2004**, *45(26)*, 8809. https://doi.org/10.1016/j.polymer.2004.10.047

[10] Mysiukiewicz O., Barczewski M.: *Journal of Polymer Research* **2020**, *27*, 1, https://doi.org/10.1007/s10965-020-02337-5

[11] Andrzejewski J., Markowski M., Barczewski M.: *Materials* **2022**, *15(15)*, 5205. https://doi.org/10.3390/ma15155205

[12] Barczewski M., Mysiukiewicz O., Lewandowski K. *et al*.: *Materials* **2020**, *13(23)*, 5436. https://doi.org/10.3390/ma13235436

[13] Barczewski M., Mysiukiewicz O., Szulc J. *et al*.: *Journal of Applied Polymer Science* **2019**, *136(24)*, 47651. https://doi.org/10.1002/app.47651

[14] Jiang L., Zhang J., Wolcott M.P.: *Polymer (Guildf)* **2007**, *48(26)*, 7632. https://doi.org/10.1016/j.polymer.2007.11.001

[15] Han J.J., Huang H.X.: *Journal of Applied Polymer Science* **2011,** *120(6)*, 3217. https://doi.org/10.1002/app.33338

[16] Imre B., Bedo D., Domján A., et al.: *European Polymer Journal* **2013**, *49(10)*, 3104. https://doi.org/10.1016/j.eurpolymj.2013.07.007
[17] Zhang W., Chen L., Zhang Y.: *Polymer (Guildf)* **2009**, *50(5)*, 1311. https://doi.org/10.1016/j.polymer.2009.01.032
[18] Cai J., Jiang J., Zhou Z. *et al*.: *Science of Advanced Materials* **2017**, *9(9)*, 1683. https://doi.org/10.1166/sam.2017.3121
[19] Piontek A., Vernaez O., Kabasci S.: *Polymers (Basel)* **2020**, *12(3)*, 605. https://doi.org/10.3390/polym12030605
[20] Bitinis N., Verdejo R., Cassagnau P. *et al*.: *Materials Chemistry and Physics* **2011**, *129(3)*, 823. https://doi.org/10.1016/j.matchemphys.2011.05.016
[21] Bitinis N., Verdejo R., Maya E.M. *et al*.: *Composites Science and Technology* **2012**, *72(2)*, 305. https://doi.org/10.1016/j.compscitech.2011.11.018
[22] Bitinis N., Sanz A, Nogales A. *et al*.: *Soft Matter* **2012**, *8*, 8990. https://doi.org/10.1039/c2sm25729g
[23] Juntuek P., Ruksakulpiwat C., Chumsamrong P. *et al*.: *Journal of Applied Polymer Science* **2012**, *125(1)*, 745. https://doi.org/10.1002/app.36263
[24] Xu C., Yuan D., Fu L. *et al*.: *Polymer Testing* **2014**, *37*, 94. https://doi.org/10.1016/j.polymertesting.2014.05.005
[25] Mustafa S.N.I.S., Man S.H.C., Hassan A. *et al*.: *AIP Conference Proceedings* **2020**, *2267*, 020062-1. https://doi.org/10.1063/5.0022360
[26] Klinkajorn J., Tanrattanakul V.: *Journal of Applied Polymer Science* **2020,** *137(34)*, 48996. https://doi.org/10.1002/app.48996
[27] Pongtanayut K., Thongpin C., Santawitee O.: *Energy Procedia* **2013**, *34*, 888. https://doi.org/10.1016/j.egypro.2013.06.826
[28] Tessanan W., Chanthateyanonth R., Yamaguchi M. *et al*.: *Journal of Cleaner Production* **2020**, *276*, 123800. https://doi.org/10.1016/j.jclepro.2020.123800
[29] Sathornluck S., Choochottiros C.: *Journal of Applied Polymer Science* **2019**, *136(48)*, 48267. https://doi.org/10.1002/app.48267
[30] Sookprasert P., Hinchiranan N.: *Journal of Materials Research* **2017**, *32*, 788. https://doi.org/10.1557/jmr.2017.9
[31] Zhao X., Hu H., Wang X. *et al*.: *RCS Advances* **2020**, *10*, 13316. https://doi.org/10.1039/D0RA01801E
[32] Huang J., Fan J., Yuan D. *et al*.: *Industrial & Engineering Chemistry Research* **2020**, *59(21)*, 9950. https://doi.org/10.1021/acs.iecr.0c00035
[33] Phetphaisit C.W., Wapanyakul W., Phinyocheep P.: *Journal of Applied Polymer Science* **2019**, *136(21)*, 47503. https://doi.org/10.1002/app.47503
[34] Moeinifar E., Otadi M., Seyfi J. *et al*.: *Polymer Bulletin* **2020**, *77*, 585. https://doi.org/10.1007/s00289-019-02766-3
[35] Ullah M.S., Yazıcı N., Wis A.A. *et al*.: *Polymer Composites* **2022**, *43(3)*, 1252. https://doi.org/10.1002/pc.26483
[36] Hebda E., Pielichowski K.: "Polyurethane/POSS Hybrid Materials" in "Polymer/POSS Nanocomposites and Hybrid Materials", (Kalia S., Pielichowski K.), Springer Cham, New York City 2018, p. 167.
[37] Zazoum B., Fréchette M., David E.: "Effect of POSS as Compatibilizing Agent on Structure and Dielectric Response of LDPE/TiO2 Nanocomposites." Materials from IEEE Conference on Electrical Insulation and Dielectric Phenomena, Ann Arbor, MI, USA, October 18–21, 2015, p.523.
[38] Kilic N.T., Can B.N., Kodal M. *et al*.: *Polymer Engineering and Science* **2020**, *60(2)*, 398. https://doi.org/10.1002/pen.25295
[39] Li S., Simon G.P., Matisons J.G.: *Journal of Applied Polymer Science* **2009**, *115(2)*, 1153. https://doi.org/10.1002/app.31225
[40] Zhao L., Li J., Li Z. *et al*.: *Composites Part B: Engineering* **2018**, *139*, 40. https://doi.org/10.1016/j.compositesb.2017.11.052
[41] Ercan Kalkan M., Karakaya N., Özkoç G.: *Polymers for Advanced Technologies* **2020**, *31(10)*, 2290. https://doi.org/10.1002/pat.4949
[42] Kilic N.T., Can B.N., Kodal M. *et al*.: *Journal of Applied Polymer Science* **2019**, *136(12)*, 47217. https://doi.org/10.1002/app.47217
[43] Bai H., Huang C, Jun L. *et al*.: *Journal of Applied Polymer Science* **2016**, *133(36)*, 43906, https://doi.org/10.1002/app.43906
[44] Bai H., Yi S., Huang C. *et al*.: *Journal of Wuhan University of Technology, Materials Science Edition* **2017**, *32*, 229. https://doi.org/10.1007/s11595-017-1585-y
[45] Ayandele E., Sarkar B., Alexandridis P.: *Nanomaterials* **2012**, (4)2, 445. https://doi.org/10.3390/nano2040445
[46] Qi Z., Zhang W., He X. *et al*.: *Composites Science and Technology* **2016**, *127*, 8. https://doi.org/10.1016/j.compscitech.2016.02.026
[47] Turgut G., Dogan M., Tayfun U. *et al*.: *Polymer Degradation and Stability* **2018**, *149*, 96. https://doi.org/10.1016/j.polymdegradstab.2018.01.025
[48] Lakshmipriya S., Anil Kumar S., Nandakumar K. *et al*.: *Polymer Composites* **2019**, *40(8)*, 3020. https://doi.org/10.1002/pc.25145
[49] Dudziec B., Marciniec B.: *Current Organic Chemistry* **2015**, *21(28)*, 2794. https://doi.org/10.2174/1385272820666151228193728
[50] Wang M., Chi H., Joshy K.S. *et al*.: *Polymers (Basel)* **2019**, *11(12)*, 2098. https://doi.org/10.3390/polym11122098
[51] Duszczak J., Mituła K., Januszewski R. *et al*.: *ChemCatChem* **2019**, *11(3)*, 1086. https://doi.org/10.1002/cctc.201801609
[52] Wang Y., Chen K., Xu C. *et al*.: *Journal of Physical Chemistry B* **2015**, *119(36)*, 12138.

https://doi.org/10.1021/acs.jpcb.5b06244
[53] Jeziórska R., Świerz-Motysia B., Szadkowska A. *et al.*: *Polimery* **2011**, *56(11-12)*, 809. https://doi.org/10.14314/polimery.2011.809
[54] Lipińska M., Toczek K., Stefaniak M.: *Materials* **2021**, *14(10)*, 2686. https://doi.org/10.3390/ma14102686
[55] Zheng M., Zhang S., Chen Y. *et al.*: *Polymer Testing* **2020**, *82*, 106324. https://doi.org/10.1016/j.polymertesting.2020.106324
[56] Yi L., Zhang J., Yang J. *et al.*: *Tribology International* **2018**, *128*, 328. https://doi.org/10.1016/j.triboint.2018.07.041
[57] Sirin H., Kodal M., Özkoç G.: *Polymer Composites* **2016**, *37(5)*, 1497. https://doi.org/10.1002/pc.23319
[58] Dandan Doğanci M.: *Journal of the Turkish Chemical Society Section A: Chemistry* **2020**, *7(3)*, 649. https://doi.org/10.18596/jotcsa.752190
[59] Hesami M., Jalali-Arani A.: *Polymer International* **2017**, *66(11)*, 1564. https://doi.org/10.1002/pi.5414
[60] Song L., He Q., Hu Y. *et al.*: *Polymer Degradation and Stability* **2008**, *93(3)*, 627. https://doi.org/10.1016/j.polymdegradstab.2008.01.014
[61] Chieng B.W., Ibrahim N.A., Yunus W.M.Z.W. *et al.*: *Polymers (Basel)* **2014**, *6(1)*, 93. https://doi.org/10.3390/polym6010093
[62] Mofokeng J.P., Luyt A.S., Tábi T. *et al.*: *Journal of Thermoplastic Composite Materials* **2012**, *25(8)*, 927. https://doi.org/10.1177/0892705711423291
[63] Torres-Huerta A.M., Del Angel-López D., Domínguez-Crespo M.A. *et al.*: *Polymer - Plastics Technology and Engineering* **2016**, *55*, 672. https://doi.org/10.1080/03602559.2015.1132433
[64] Xu T., Jia Z., Luo Y. *et al.*: *Applied Surface Science* **2015**, *328*, 306. https://doi.org/10.1016/j.apsusc.2014.12.029
[65] Hamzah R., Bakar M.A., Khairuddean M. *et al.*: *Molecules* **2012**, *17(9)*, 10974. https://doi.org/10.3390/molecules170910974
[66] Van Zyl A.J.P., Graef S.M., Sanderson R.D. *et al.*: *Journal of Applied Polymer Science* **2003**, *88(10)*, 2539. https://doi.org/10.1002/app.12061
[67] Gan S.-N., Hamid Z.A.: *Polymer (Guildf)* **1997**, *38(8)*, 1953. https://doi.org/10.1016/S0032-3861(96)00710-0

Received 10 X 2023.